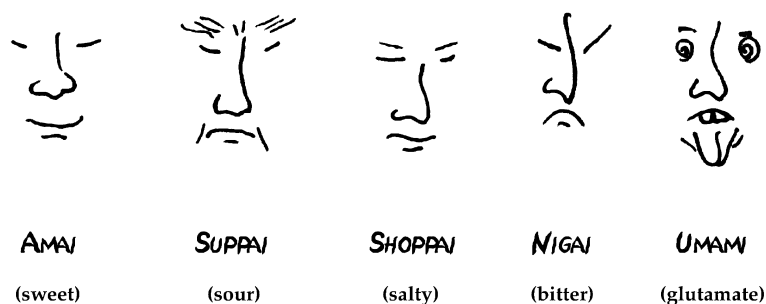# Molecular mechanisms of taste transduction*

Robert F. Margolskee[‡]

Howard Hughes Medical Institute, Department of Physiology and Biophysics, 1425 Madison Avenue, Box 1677, Mount Sinai School of Medicine, New York, NY 10029, USA

Abstract: Taste transduction is a specialized form of signal transduction by which taste receptor cells (TRCs) encode at the cellular level information about chemical substances encountered in the oral environment (so-called tastants). Bitter and sweet taste transduction pathways convert chemical information into a cellular second messenger code utilizing cyclic nucleotides, inositol trisphosphate, and/or diacyl glycerol. These messengers are components of signaling cascades that lead to TRC depolarization and Ca^{++} release. Bitter and sweet taste transduction pathways typically utilize taste-specific or taste-selective seven transmembrane-helix receptors, G proteins, effector enzymes, second messengers, and ion channels. The structural and chemical diversity of tastants has led to the need for multiple transduction mechanisms. Through molecular cloning and data mining, many of the receptors, G proteins, and effector enzymes involved in transducing responses to bitter and sweet compounds are now known. New insights into taste transduction and taste coding underlying sweet and bitter taste qualities have been gained from molecular cloning of the transduction elements, biochemical elucidation of the transduction pathways, electrophysiological analysis of the function of taste cell ion channels, and behavioral analysis of transgenic and knockout models.

INTRODUCTION

Figure 1 is based on a delightful silkscreen image by John Lennon in which he presented a graphical depiction of four categories of human taste sensation: *amai* (sweet), *suppai* (sour), *shoppai* (salty), *karai* (hot-spicy), and *nigai* (bitter). I have modified this image to present the more typical representation of human taste sensation categorized as sweet, sour, salty, bitter, and *umami* (glutamate). Our ability to

AMAI	SUPPAI	SHOPPAI	NIGAI	UMAMI
(sweet)	(sour)	(salty)	(bitter)	(glutamate)

Fig. 1 Schematic representation of human taste qualities. Psychophysical studies suggest that human taste sensation can be divided into five distinct categories: *amai* (sweet), *suppai* (sour), *shoppai* (salty), *nigai* (bitter), and *umami* (glutamate). Modified from the original silkscreen by John Lennon.
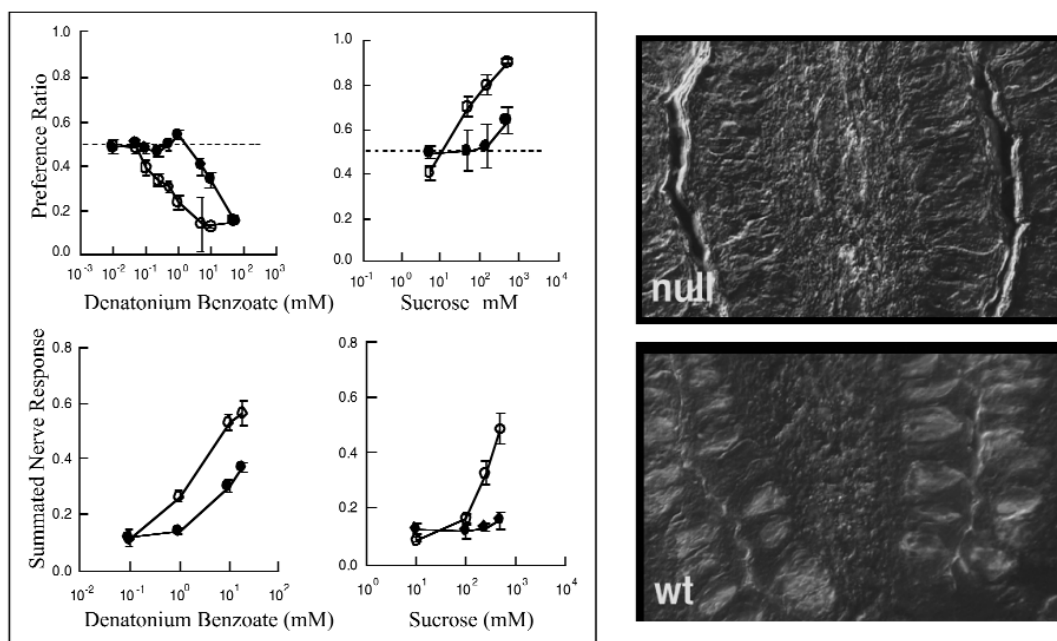
identify different-tasting substances provides us with a means to seek out foodstuffs with nutritive value, while avoiding spoiled foods or poisonous substances. This review presents recent research from my laboratory and others on the transduction elements and signaling mechanisms that underlie bitter and sweet taste transduction.

The sensations of bitter and sweet tastes are initiated by the interaction of tastants with G protein-coupled receptors (GPCRs) in the apical membranes of taste receptor cells (TRCs). TRCs are specialized epithelial cells with many neuronal properties, including the ability to depolarize and form synapses. TRCs are typically clustered in groups of ~100 within taste buds. The convoluted apical surface of TRCs, which makes contact with the oral cavity, is rich in microvilli-containing GPCRs, ion channels, and other transduction elements. The basolateral aspect of TRCs contains ion channels and synapses with afferent taste nerves.

BITTER TRANSDUCTION

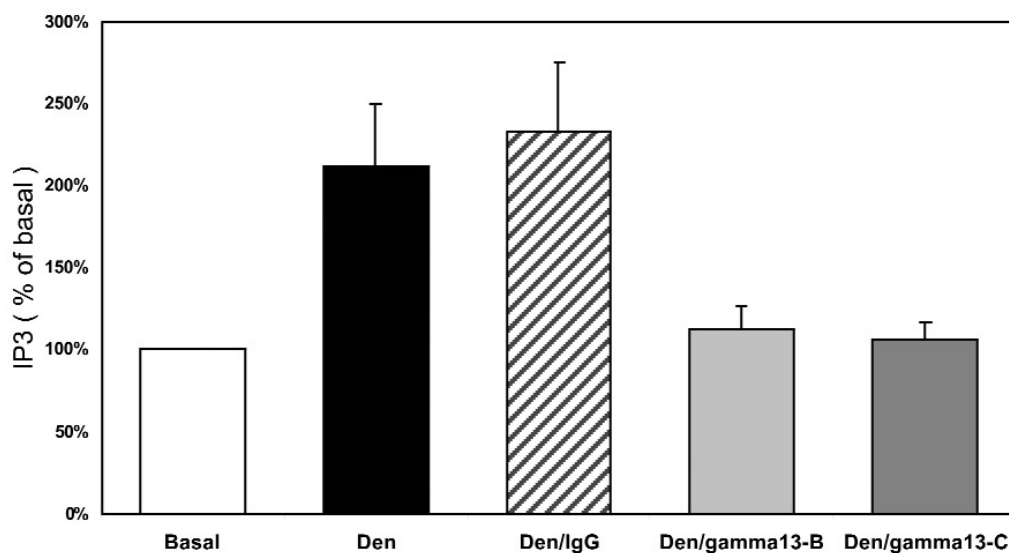### G proteins and G protein-activated effector enzymes

α-Gustducin is an α-transducin-like G protein α-subunit selectively expressed in ~25 % of TRCs [1,2]. α-Gustducin knockout mice show markedly reduced behavioral and nerve responses to several bitter compounds (e.g., denatonium benzoate and quinine sulfate) (see Fig. 2) [3]. Quench-flow studies from

Fig. 2 Gustducin knockout mice have diminished behavioral and electrophysiological responses to both bitter and sweet compounds. **Left, upper panels**: mean preference ratios from 48-h two-bottle preference tests of gustducin knockout mice (filled circles; $n = 12$) compared to wild-type littermates (open circles; $n = 12$). Only male mice were used, presentation of denatonium benzoate (0.01, 0.05, 0.1, 0.25, 0.5, 1, 5, 10, 50 mM) and sucrose (5, 50, 150, 500 mM) was in ascending order; tastants were presented vs. distilled water. **Left, lower panels**: summated chorda tympani nerve responses of gustducin knockout mice (filled circles; $n = 6$) compared to wild-type littermates (open circles; $n = 6$). Only male mice were used. Responses to denatonium benzoate (0.1, 1, 10, 20 mM) and sucrose (10, 100, 250, 500 mM) were normalized to that to 100 mM NH_4Cl. **Right panels**: indirect immunofluorescent detection of α-gustducin demonstrates its absence from the knockout mice (null) and presence in taste buds from wild-type mice (wt). Modified from Wong et al. [3].

Andrew Spielman's laboratory have shown that many bitter compounds lead to a gustducin-mediated decrease in taste tissue cyclic nucleotide (cNMP) levels [4]. The G protein-activated enzyme involved in these responses has recently been identified as phosphodiesterase type 1A (PDE1A) [Bakre, Glick, Rybalkin, Max, Beavo, and Margolskee, unpublished].

In response to bitter compounds, gustducin's $\beta\gamma$-subunits (Gβ3 and Gγ13) mediate an increase in taste tissue levels of inositol trisphosphate (IP$_3$) and diacyl glycerol (DAG) [5,6]. Antibodies directed against Gβ3, Gγ13, or PLCβ2 block this response (see Fig. 3) [5–7], implicating all three of these proteins in bitter taste responses. Consistent with their role in an IP$_3$/DAG taste-signaling pathway, α-gustducin, Gβ3, Gγ13, and PLCβ2 are co-expressed in large part in TRCs [8,9].
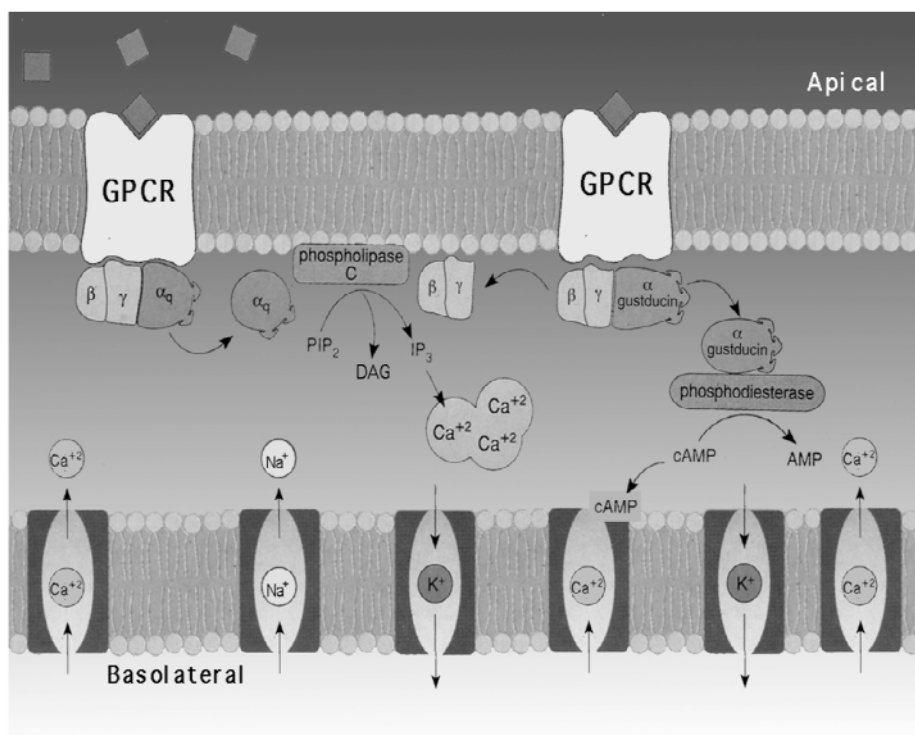

Fig. 3 Bitter-induced IP$_3$ production in mouse taste tissue is mediated by Gγ13. Mouse taste tissue samples were stimulated with buffer alone (Basal), 1 mM denatonium (Den), or with 1 mM denatonium plus various antibodies [normal IgG (Den/IgG), anti-Gγ13-B (Den/gamma 13-B), anti-Gγ13-C (Den/gamma 13-C)], then quenched at 50 msec in a quench-flow module. The anti-Gγ13 antibody was directed against aa 18-32 of Gγ13; the anti-Gγ13-C antibody was directed against aa 47-59 of Gγ13. Modified from Huang et al. [5].

Receptors

"Data mining" of the NCBI (National Center for Biotechnology Information) DNA sequence databases was used to identify a ~25 member multigene family of TRC-expressed GPCRs, named T2Rs or TRBs [10,11]. In rat and mouse, T2R/TRB receptors are expressed in ~15–20 % of TRCs in taste buds of the circumvallate and foliate papillae and the palate, but in very few TRCs in fungiform papillae [10]. Based on in situ hybridization with mixed vs. individual T2R/TRB probes, it was concluded that most T2R/TRB receptors are expressed in the same TRCs [10,11]. T2R/TRB receptors are only found in TRCs positive for expression of gustducin [10]. One murine T2R/TRB receptor (mT2R5), when expressed in heterologous cells, responded to bitter cycloheximide at a concentration comparable to the murine threshold for aversion [12]. mT2R5 was shown in vitro to couple selectively to α-gustducin vs. other G protein α-subunits.

Transduction pathways

Gustducin heterotrimers that have been activated by bitter-stimulated T2R/TRB receptors mediate two responses in TRCs: a decrease in cNMPs via α-gustducin and a rise in IP$_3$/DAG via βγ-gustducin. The subsequent steps in the α-gustducin-PDE-cNMP pathway may depend upon protein kinases to regulate TRC ion channel activity, or cNMP levels may regulate directly the activity of cNMP-gated [13] and cNMP-inhibited [14] ion channels expressed in TRCs. The subsequent steps in the βγ-gustducin-PLC-IP$_3$/DAG pathway are thought to be activation of IP$_3$ receptors and release of Ca^{++} from internal stores followed by neurotransmitter release [15]. These pathways are diagrammed in Fig. 4.

Fig. 4 Proposed transduction mechanisms in vertebrate taste receptor cells underlying bitter taste. Bitter compounds activate G protein-coupled receptors (GPCRs) identified as T2R/TRB receptors. T2R/TRB receptors activate gustducin heterotrimers. Activated α-gustducin stimulates phosphodiesterase to hydrolyze cAMP; the decreased cAMP may disinhibit cyclic nucleotide-inhibited channels to elevate intracellular Ca^{2+}. Activated gustducin's Gβγ subunits (β3γ13) activate phospholipase C to generate IP$_3$ which leads to release of Ca^{2+} from internal stores.

SWEET TRANSDUCTION
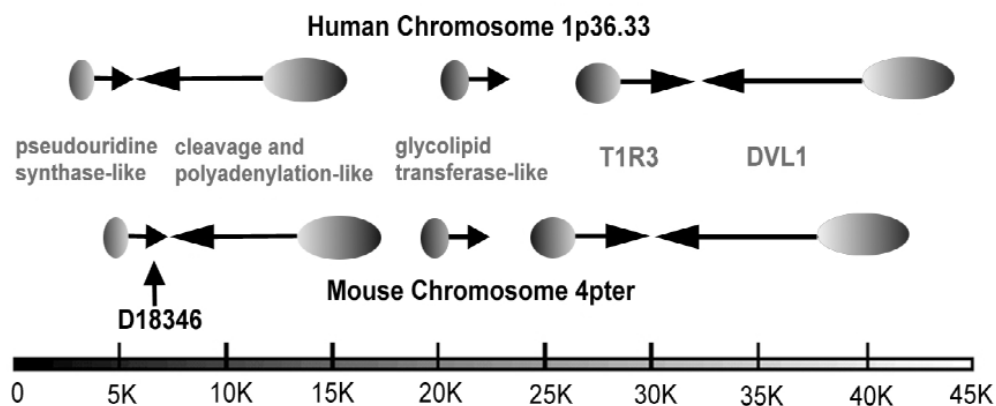
G proteins and G protein-activated effector enzymes

Several biochemical and electrophysiological studies have implicated G$_s$, adenylyl cylcase, and cAMP in TRC responses to sweet tastants [reviewed in 16]. In one study, PLCβ2 and IP$_3$/DAG were implicated in sweet taste [15]. Gustducin may be involved in sweet as well as in bitter responses: α-gustducin knockout mice show diminished behavioral and/or electrophysiological responses to many sweet compounds, including sucrose and the artificial sweeteners saccharin and SC45647 (see Fig. 2) [3]. It has

not yet been determined which G protein α- and βγ-subunits couple with the T1r3 sweet receptor. Double in situ hybridization and double immunofluorescence indicate that in circumvallate papillae taste buds only 10–15 % of T1r3-expressing TRCs also express α-gustducin; however, in fungiform taste buds the majority of T1r3-epxressing TRCs also express α-gustducin [17; Zou, Damak, and Margolskee, unpublished; Kitagawa, Kusakabe, Miura, Ninomiya, and Hino, personal communication].

Receptors

The murine *Sac* locus is the major genetic factor that determines differences between sweet-preferring and sweet-indifferent strains of mice [18–21]. *Sac* determines both behavioral and electrophysiological responsiveness to saccharin, sucrose, and other sweeteners [22,23], suggesting that it acts distally and might encode a taste receptor. *Sac* has been mapped to the distal end of mouse chromosome 4 [22–25].
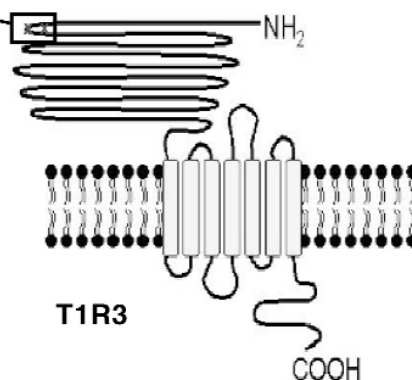
Based on the earlier genetic mapping and recent data mining of human and mouse DNA sequence databases, the receptors underlying sweet taste have now been identified [17,26–28]. To identify the *Sac* gene, all genes present within a region of ~1 million bp of the sequenced human genome syntenous to the *Sac* region of mouse were identified and ordered into a contiguous stretch of DNA (a "contig") (see Fig. 5) [26]. From this search, T1R3 (human taste receptor family 1, member 3), a previously unknown GPCR, and the only GPCR in this region of the genome, was identified as the most likely candidate for *Sac*. T1R3 is ~30 % related to T1R1 and T1R2, two "orphan" GPCRs selectively expressed in TRCs [29]. T1R3 was also identified independently in searches for novel TRC-expressed GPCRs that mapped to the region of the human genome syntenous to the murine *Sac* region [17,28], as well as by an RT-PCR search for novel taste receptors [27]. As befits a taste receptor, T1R3 and/or the murine ortholog (T1r3) were shown to be expressed selectively in TRCs within fungiform, foliate, and circumvallate papillae [17,26–28].
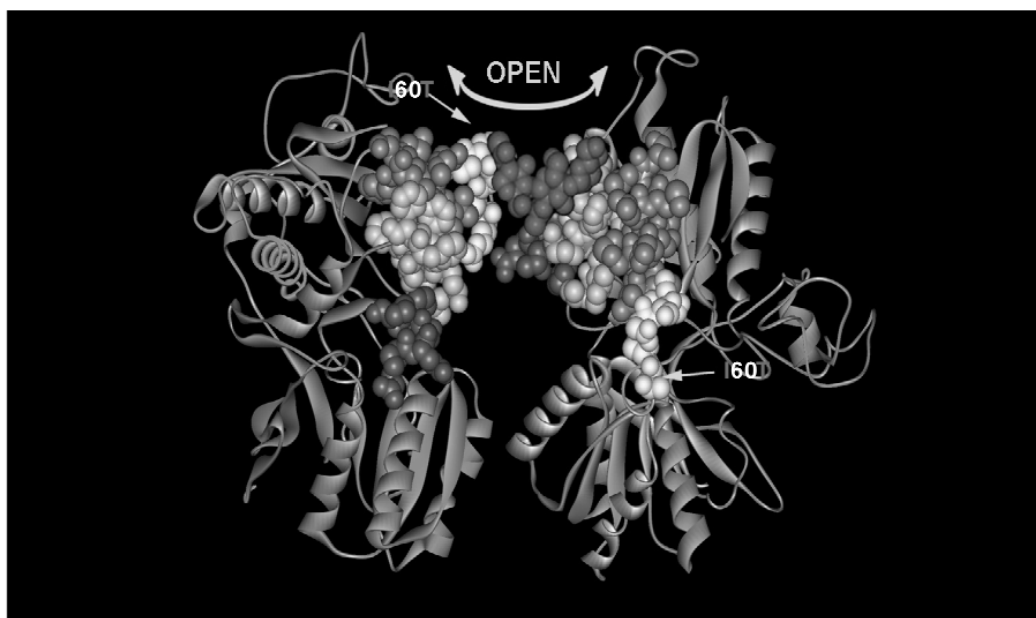

Fig. 5 Data-mining identification of candidate genes in the region of the *Sac* locus. Syntenic regions between human 1p36.33 and mouse 4pter chromosomal regions near the mouse *Sac* locus are shown. Shaded circles indicate the approximate location of the predicted start codons for each gene; arrows indicate the full span of each gene including both introns and exons; arrowheads indicate the approximate location of each polyadenylation signal. Genes indicated by lowercase letters were predicted by Genscan and named according to their closest homolog. Genes indicated by capital letters (T1R3 and DVL1) were experimentally identified and verified. The mouse marker D18346 indicated is closely linked to the *Sac* locus and lies within the predicted pseudouridine synthase-like gene. The region displayed corresponds to ~45 000 bp; the bottom scale marker indicates kilobases (K). Modified from Max et al. [26].

By comparing the sequence of T1r3 from several independently derived strains of mice, eight amino acid polymorphisms were identified, however, only two of these polymorphisms differentiated all taster strains of mice from all non-taster strains (see Fig. 6) [17,26–28,30]. These two polymorphisms occur within a specific portion of the *N*-terminal extracellular region of T1r3 that is predicted to be involved in GPCR dimerization. T1r3 from non-tasters is predicted to contain an extra *N*-terminal glycosylation site that according to models of T1r3's structure would preclude its hetero- or homodimerization (see Fig. 7) [26]. Confirmation that T1R3 is *Sac* has come recently from the conversion of non-taster mice into tasters by the transgenic expression of T1R3 from a taster strain [30; Rong, He, Damak and Margolskee, unpublished]. Heterologous expression of T1r3 in combination with T1r2 demonstrated that this heterodimer comprises a functional taste receptor responsive to several natural and artificial sweeteners [30]. Heterologous expression of T1r3 or T1r2 alone did not yield sweet-responsive cells, suggesting that a T1r3/T1r2 heterodimeric form is required to manifest a functional sweet receptor. Heterologous expression of T1r3 in combination with T1r1 led to responsiveness to glutamate and other umami compounds [31,32].

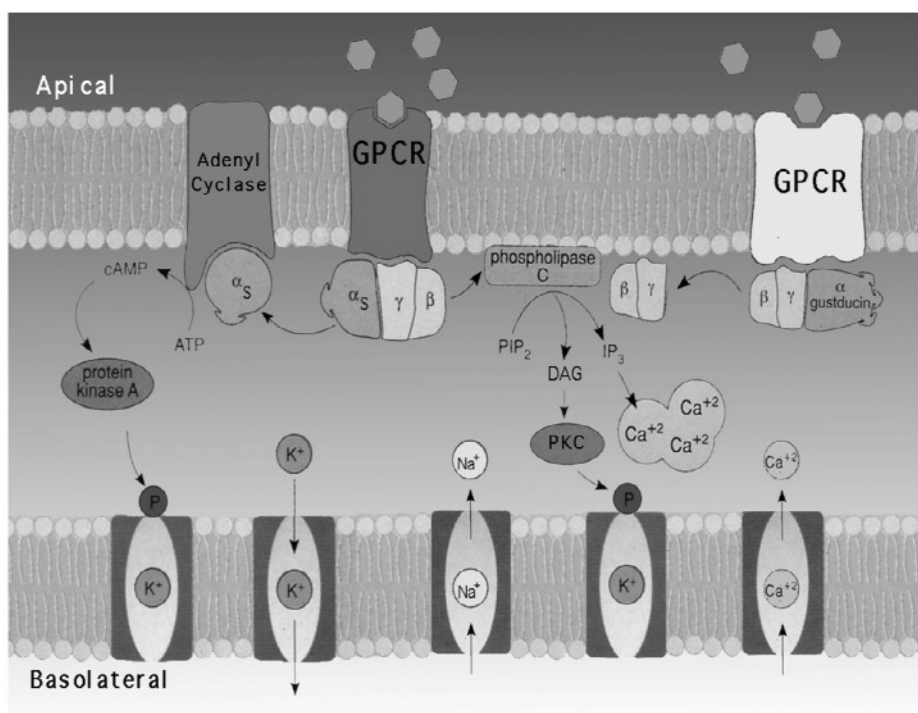| Nucleotide position	135	163	179	182	186	264	270	312	652	692	965	969	1300	2647	2689
C57BL/6J	A	A	T	C	C	-	A	T	T	T	A	C	G	T	T
FVB/N, SWR, ST/bJ	A	A	T	T	T	G	G	C	T	C	G	T	A	C	C
Non-taster strains	G	G	C	T	T	G	G	C	C	C	G	C	A	T	C
Coding change	s	T55A	I60T	P61L	s	i	i	s	i	s	s	C261R	R371Q	S692L	I706T

Fig. 6 T1r3 nucleotide sequence differences between eight inbred mouse strains. All non-taster strains showed identical sequences and were grouped in one row. Two alleles were noted in the four taster strains. The bottom row displays the inferred amino acid sequence. The amino acid immediately after the position number is always from the non-tasters, while that immediately before the position number is from whichever tasters differed at that position from the non-tasters. The two columns in bold represent positions where all tasters differed from all non-tasters and where the differences in nucleotide sequence result in amino acid substitutions. These two taster to non-taster polymorphisms are T55A and I60T. Nucleotide differences that do not alter the encoded amino acid are indicated as *s*: silent. Nucleotide differences within introns are indicated as *i*: intron. The approximate location of T55A and I60T are indicated in the extreme *N*-terminus of the amino-terminal domain of murine T1r3. Modified from Max et al. [26].

Fig. 7 The three-dimensional structure of the amino-terminal domain (ATD) of murine T1r3. The model, based on the solved structure of the ATD of mGluR1 [see ref. 26], shows a T1r3 homodimer. The T1r3 dimer is viewed from the side. The two monomers have been spread apart (indicated by the double headed arrow) to reveal the contact surface. A space-filling representation of three glycosyl moieties (*N*-acetyl-galactose-*N*-acetyl-galactose-Mannose) has been added at the novel predicted site of glycosylation of non-taster mT1R3. Note that the addition of even three sugar moieties at this site is sterically incompatible with dimerization. Regions of mT1R3 corresponding to those of mGluR1 involved in dimerization are shown by space filling amino acids. The portions of the two molecules outside of the dimerization region are represented by a backbone tracing. The two polymorphic amino acid residues of T1r3 that differ in taster vs. non-taster strains of mice are within the predicted dimerization interface nearest the amino terminus. The additional *N*-glycosylation site at amino acid 58 unique to the non-taster form of T1r3 is indicated in each panel by the straight arrows. Modified from Max et al. [26].

Transduction pathways

Based on biochemical and electrophysiological studies of taste cells [15,33–40] two models for sweet transduction have been proposed (see Fig. 8). First, a GPCR-G_s-cAMP pathway: sucrose and other sugars activate G_S via one or more coupled GPCRs; receptor-activated $G\alpha_S$ activates adenylyl cyclase (AC) to generate cAMP; cAMP may act directly to cause cation influx through cNMP gated channels, or act indirectly to activate protein kinase A, which phosphorylates a basolateral K^+ channel, leading to closure of the channel, depolarization of the taste cell, voltage-dependent Ca^{++} influx, and neurotransmitter release. Second, a GPCR-G_q/$G\beta\gamma$-IP_3 pathway: artificial sweeteners presumably bind to and activate one or more GPCRs coupled to PLCβ2 by either the α subunit of G_q or by $G\beta\gamma$ subunits; activated $G\alpha_q$ or released $G\beta\gamma$ activates PLCβ2 to generate IP_3 and DAG; IP_3 and DAG elicit Ca^{++} release from internal stores, leading to depolarization of the TRC and neurotransmitter release. These two pathways (diagrammed in Fig. 8) apparently coexist in the same TRCs [15].

Fig. 8 Proposed transduction mechanisms in vertebrate taste receptor cells underlying sweet taste. Artificial sweeteners activate GPCRs (T1R heterodimers) apparently linked via heterotrimeric gustducin to phospholipase C. Activated gustducin's Gβγ subunits (β3γ13) activate phospholipase C to generate IP_3, which leads to release of Ca^{2+} from internal stores. Sugars activate T1R heterodimers apparently linked via heterotrimeric Gs to adenylyl cyclase. Elevated levels of cAMP produced by the activated adenylyl cyclase may lead to inhibition of basolateral K^+ channels via cAMP-activated protein kinase A phospohorylation of these channels.

ACKNOWLEDGMENTS

REFERENCES

1. S. K. McLaughlin, P. J. McKinnon, R. F. Margolskee. *Nature* **357**, 563–569 (1992).
2. J. D. Boughter, Jr., D. W. Pumplin, C. Yu, R. C. Christy, D. V. Smith. *J. Neurosci.* **17**, 2852–2858 (1997).
3. G. T. Wong, K. S. Gannon, R. F. Margolskee. *Nature* **381**, 796–800 (1996).
4. W. Yan, G. Sunavala, S. Rosenzweig, M. Dasso, J. G. Brand, A. I. Spielman. *Am. J. Physiol.* **280**, C742–C751 (2001).
5. L. Huang, Y. G. Shanker, J. Dubauskaite, J. Z. Zheng, W. Yan, S. Rosenzweig, A. I. Spielman, M. Max, R. F. Margolskee. *Nat. Neurosci.* **2**, 1055–1062 (1999).
6. P. Rossler, I. Boekhoff, E. Tareilus, S. Beck, H. Breer, J. Freitag. *Chem. Senses* **25**, 413–421 (2000).
7. P. Rossler, C. Kroner, J. Freitag, J. Noe, H. Breer. *Eur. J. Cell Biol.* **77**, 253–261 (1998).
8. T. R. Clapp, L. M. Stone, R. F. Margolskee, S. C. Kinnamon. *BMC Neurosci.* **6**, 2–10 (2001).

9. M. A. Miyoshi, K. Abe, Y. Emori. *Chem. Senses* **26**, 259–265 (2001).
10. E. Adler, M. A. Hoon, K. L. Mueller, J. Chandrashekar, N. J. P. Ryba, C. S. Zuker. *Cell* **10**, 693–702 (2000).
11. H. Matsunami, J.-P. Montmayeur, L. B. Buck. *Nature* **404**, 601–604 (2000).
12. J. Chandrashekar, K. L. Mueller, M. A. Hoon, E. Adler, L. Feng, W. Guo, C. S. Zuker, N. J. P. Ryba. *Cell* **100**, 703–711 (2000).
13. T. Misaka, Y. Kusakabe, Y. Emori, T. Gonoi, S. Arai, K. Abe. *J. Biol. Chem.* **272**, 22623–22629 (1997).
14. S. S. Kolesnikov and R. F. Margolskee. *Nature* **376**, 85–88 (1995).
15. S. J. Bernhardt, M. Naim, U. Zehavi, B. Lindemann. *J. Physiol.* **490**, 325–336 (1996).
16. T. A. Gilbertson, S. Damak, R. F. Margolskee. *Curr. Opin. Neurobiol.* **10**, 519–527 (2000).
17. J. P. Montmayeur, S. D. Liberles, H. Matsunami, L. B. Buck. *Nat. Neurosci.* **4**, 492–498 (2001).
18. I. E. Lush, N. Hornigold, P. King, J. P. Stoye. *Genet. Res.* **66**, 167–174 (1995).
19. J. L. Fuller. *J. Hered.* **65**, 33–36 (1974).
20. I. E. Lush. *Genet. Res.* **53**, 95–99 (1989).
21. C. G. Capeless and G. Whitney. *Chem. Senses* **20**, 291–298 (1995).
22. Y. Ninomiya, N. Sako, H. Katsukawa, M. Funakoshi. In *Chemical Senses, Vol. 3, Genetics of Perception and Communication,* C. J. Wysocki and M. R. Kare (Eds.), pp. 267–278, Marcel Dekker, New York (1991).
23. A. A. Bachmanov, D. R. Reed, Y. Ninomiya, M. Inoue, M. G. Tordoff, R. A. Price, G. K. Beauchamp. *Mamm. Genome* **8**, 545–548 (1997).
24. D. A. Blizzard, B. Kotlus, M. E. Frank. *Chem. Senses* **24**, 373–385 (1999).
25. X. Li, M. Inoue, D. R. Reed, T. Huque, R. B. Puchalski, M. G. Tordoff, Y. Ninomiya, G. K. Beauchamp, A. A. Bachmanov. *Mamm. Genome* **12**, 13–16 (2001).
26. M. Max, Y. G. Shanker, L. Huang, M. Rong, Z. Liu, F. Campagne, H. Weinstein, S. Damak, R. F. Margolskee. *Nat. Genet*. **28**, 58–63 (2001).
27. M. Kitagawa, Y. Kusakabe, H. Miura, Y. Ninomiya, A. Hino. *Biochem. Biophys. Res. Commun.* **283**, 236–242 (2001).
28. E. Sainz, J. N. Korley, J. F. Battey, S. L. Sullivan. *J. Neurochem.* **77**, 896–903 (2001).
29. M. A. Hoon, E. Adler, J. Lindemeier, J. F. Battey, N. J. P. Ryba, C. S. Zuker. *Cell* **96**, 541–551 (1999).
30. G. Nelson, M. A. Hoon, J. Chandrashekar, Y. Zhang, N. J. P. Ryba, C. S. Zuker. *Cell* **106**, 381–390 (2001).
31. X. Li, L. Staszewski, H. Xu, K. Durick, M. Zoller, F. Adler. *Proc. Natl. Acad. Sci USA* **99**, 4692–4696 (2002).
32. G. Nelson, J. Chandrashekar, M. A. Hoon, L. Feng, G. Zhao, N. J. Ryba, C. S. Zuker. *Nature* **416**, 199–202 (2002).
33. B. J. Striem, U. Pace, U. Zehavi, M. Naim, D. Lancet. *Biochem. J.* **260**, 121–126 (1989).
34. B. J. Striem, M. Naim, B. Lindemann. *Cell Physiol. Biochem.* **1**, 46–54 (1991).
35. M. Naim, T. Ronen, B. J. Striem, M. Levenson, U. Zehavi. *Comp. Biochem. Physiol.* **100B**, 455–458 (1991).
36. K. Tonosaki and M. Funakoshi. *Nature* **331**, 354–356 (1988).
37. P. Avenet, F. Hofmann, B. Lindemann. *Nature* **331**, 351–354 (1988).
38. P. Avenet, F. Hofmann, B. Lindemann. *Comp. Biochem. Biophysiol.* **90A**, 681–685 (1988).
39. T. A. Cummings, J. Powell, S. C. Kinnamon. *J. Neurophys.* **70**, 2326–2336 (1993).
40. T. A. Cummings, C. Daniels, S. C. Kinnamon. *J. Neurophys.* **75**, 1256–1263 (1996).